

# Evaluation of respiratory bronchiolitis nodules with maximum intensity projection images

Hüseyin Alper Kızıoğlu<sup>1\*</sup> , Murat Beyhan<sup>1</sup> , Erkan Gökçe<sup>1</sup> 

## SUMMARY

**OBJECTIVE:** Respiratory bronchiolitis is a disease associated with heavy smoking. Computed tomography in this disease often shows symmetrical and bilaterally ill-defined circumscribed centriacinar micronodular involvement in the upper-middle lobes. The maximum intensity projection method is a kind of image processing method and provides a better evaluation of nodules and vascular structures. Our study aimed to show whether maximum intensity projection images increase the diagnostic accuracy in the detection of micronodules in respiratory bronchiolitis.

**METHODS:** Two radiologists with different experiences (first reader: 10-year radiologist with cardiothoracic radiology experience and second reader: nonspecific radiologist with 2 years of experience) reviewed images of patients whose respiratory bronchiolitis diagnosis was supported by clinical findings. The evaluation was done independently of each other. Both conventional computed tomography images and maximum intensity projection images of the same patients were examined. The detection rates on conventional computed tomography and maximum intensity projection images were then compared.

**RESULTS:** A total of 53 patients were evaluated, of whom 48 were men and 5 were women. The first reader detected centriacinar nodules in 42 (79.2%) patients on conventional computed tomography and centriacinar nodules in all 53 (100%) patients on maximum intensity projection images. The second reader detected centriacinar nodules in 12 (22.6%) patients on conventional computed tomography images and in 48 (90.6%) patients on maximum intensity projection images. For the less experienced reader, the detection rate of micronodules in respiratory bronchiolitis in maximum intensity projection images increased statistically significantly ( $p < 0.001$ ).

**CONCLUSION:** Maximum intensity projection images in respiratory bronchiolitis increase the detectability of micronodules independently of the experience of the radiologist.

**KEYWORDS:** Bronchiolitis. Lung. Multiple pulmonary nodules. Smoking.

## INTRODUCTION

Smoking is one of the leading causes of preventable death worldwide. Smoking mainly causes lung cancer and chronic obstructive pulmonary disease in the lung. In addition, smoking both increases the susceptibility to lung infection and accelerates lung fibrosis. Smoking also causes some non-neoplastic lung diseases such as desquamative interstitial pneumonia (DIP), respiratory bronchiolitis (RB), RB-associated interstitial lung disease (RB-ILD), and Langerhans cell histiocytosis (LCH)<sup>1</sup>.

Respiratory bronchiolitis is one of the non-neoplastic lung diseases associated with smoking. Histopathological presence in the lungs of smokers was first demonstrated in 1974<sup>2</sup>. The main histological finding in RB is peribronchial pigmented macrophage accumulation. Although classical computed tomographic (CT) findings of RB are variable, ill-defined centrilobular micronodules and bronchial wall thickenings are frequently detected<sup>3</sup>. In addition, areas of varying degrees of ground glass density can be seen on CT. Hypersensitivity pneumonia should

be considered in the radiological differential diagnosis of RB. The absence of a positive relationship between hypersensitivity pneumonia and smoking, the presence of a history of organic antigen exposure, and lymphocytosis in the bronchoalveolar lavage (BAL) fluid contribute to its differentiation from RB. Nonspecific findings are seen in BAL in RB<sup>1</sup>.

Computed tomography technology has shown a rapid development process in recent years. The maximum intensity projection (MIP) method, which is a not very new reconstruction technique, is especially helpful in the evaluation of pulmonary vascular structures and micronodules<sup>4</sup>. In this technique, voxels with the highest attenuation value for each slice are projected onto a two-dimensional image. MIP and minimum intensity projection (MinIP) images are a simplified version of the volume rendering technique. MIP images are particularly suitable for analyzing superposed complex anatomical structures with small volumes. In the literature, there are studies comparing conventional CT and MIP images in

<sup>1</sup>Tokat Gaziosmanpaşa University, Faculty of Medicine, Department of Radiology – Tokat, Turkey.

\*Corresponding author: alperkzloglu@hotmail.com

Conflicts of interest: the authors declare there is no conflicts of interest. Funding: none.

Received on July 04, 2023. Accepted on August 26, 2023.

the detection of micronodules<sup>4,5</sup>. However, there is no study in the literature showing the diagnostic contribution of MIP examination by radiologists with different experiences to a specific micronodular disease. The main indications for the use of MIP images in the lung window are that it is used to evaluate mild form micronodular lung infiltrates, bronchial diseases, pulmonary microcirculation anomalies, and mild form lung heterogeneity<sup>6</sup>.

In our study, it is evaluated whether MIP images, which are a known technique in the detection of RB and RB-ILD, which are common in the community and cause a relatively mild clinical course associated with smoking, are more sensitive than conventional images.

## METHODS

The study was carried out retrospectively and the study was started after the approval of the local ethics committee dated 11.03.2022 and numbered 22-KAEK-237. Our study was carried out according to the "Helsinki Declaration."

### Case selection

Patients who underwent high-resolution thorax CT (HRCT) between January 2019 and September 2022 and who had a smoking history were included in our study. Lung biopsy was not performed on the patients. Patients with clinical and radiological findings suitable for RB and RB-ILD were included in the study. Conditions mimicking RB and RB-ILD images were not included in the study. For this purpose, cases with lymphocytosis in BAL fluid and with organic antigen exposure were not included in the study even if they had appropriate clinical and radiological findings. In addition, other diseases with micronodular involvement were not included in the study. For this purpose, clinical cases suitable for miliary tuberculosis were excluded. Also, cases of sarcoidosis were not included. In addition, due to the possibility of pneumoconiosis, attention was paid to occupational anamnesis, and cases with a history of exposure were excluded. In addition, patients whose HRCT examination was not of optimal quality (not breathing properly, patients in motion, imaging that did not cover the entire lung in the examination area) were not included in the study.

### High-resolution thorax computed tomography technique and protocol

The images of the patients were obtained using a 64-slice CT device (GE Optima CT660) with a speed of 0.5 s in a helical scanning type bone algorithm with a section thickness of 0.625 mm. In technical parameters, it produced 350

milliamperes-seconds (mAs) and 120 kilovoltage peak (kVp) X-ray. Collimation was of 1 mm thick. The mean X-ray exposure time was 3.13 s. Although the field of view ratio was manually adjusted from patient to patient, it was adjusted according to the Large Body option before the examination. The dose length product (DLP) body was set to 386.74 mGy×cm at 32 cm Phantom. The examination was obtained from the level of the thyroid gland in the neck region to the inferior of the costophrenic sinuses, while the patient was in the supine position and in deep inspiration. No contrast agent was used for the examination. Adjustment of MIP images was obtained by automatically reconstructing 10-mm slab thickness axial and coronal images in the workstation.

### Image evaluation

The images were analyzed by two radiologists with different experiences (first reader with 10 years of experience in cardiothoracic radiology and second reader with 2 years of experience as nonspecific radiologist). Images were evaluated from a 21.3-inch 3MP IPS Screen medical monitor via Sectra IDS 7 PACS (Picture Archiving and Communication Systems). Both readers reviewed independently. First, whether they detected centriacinar nodules for each patient on conventional CT images was recorded. One month after the conventional CT images of all patients were examined, MIP images were examined. Then, whether they detected centriacinar nodules on MIP images was recorded. Conventional CT and MIP images were evaluated by both radiologists on axial and coronal images. Conventional and MIP images were evaluated at the same window level (WL) and same window width (WW) in the lung parenchyma window (WW=1500 HU, WL= -650 HU).

### Statistical analysis

The Windows SPSS 20 package program was used for the statistical analysis of data. Categorical measurements were summarized as numbers and percentages, and continuous measurements were summarized as mean, deviation, and minimum-maximum. The normality of distributions was evaluated using the Kolmogorov-Smirnov and Shapiro-Wilk *W* tests. The independent samples *t*-test was used as our data showed a normal distribution. *p*<0.05 was considered statistically significant. Detection rates of centriacinar nodules for the first and second readers were examined using the McNemar test.

## RESULTS

A total of 53 patients were included in our study, of whom 48 (90.6%) were males and 5 (9.4%) were females. The mean

age of the patients was calculated as  $61.6 \pm 11.6$  (38–88 years). All of the patients were smokers, and the average smoking rate was  $34 \pm 11.4$  packs/year (20–80 packs/year). The mean age of the male patients was  $61.2 \pm 11.6$  years, and the mean smoking rate was  $34.9 \pm 11.6$  packs/year. The mean age of the female patients was  $66 \pm 11.7$  years, and the mean smoking rate was  $26 \pm 5.4$  packs/year (Table 1). There was no statistically significant difference between male and female patients for age and smoking variables in RB patients ( $p=0.386$  and  $p=0.1$ , respectively).

The first reader (a cardiothoracic radiologist with 10 years of experience) detected centriacinar nodules in 42 (79.2%) of 53 patients on conventional CT images and centriacinar nodules in all 53 (100%) patients on MIP images (Figures 1A and B).

**Table 1.** Number of patients, smoking, and age.

	Number (%)	Age (years) $\pm$ SD	Smoking (packs/year) $\pm$ SD
Male	48 (90.6)	$61.2 \pm 11.6$	$34.9 \pm 11.6$
Female	5 (9.4)	$66 \pm 11.7$	$26 \pm 5.4$
Total	53 (100)	$61.6 \pm 11.6$	$34 \pm 11.4$

SD: standard deviation.

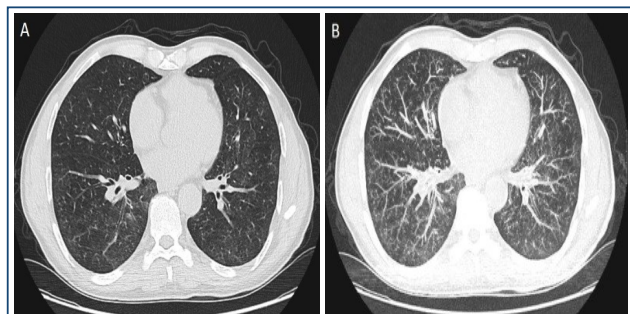


**Figure 1.** (A) In a 57-year-old male patient with a 35 packs/year smoking history, ill-defined centriacinar nodules were detected on a conventional axial computed tomography scan. (B) Centriacinar nodules are more demonstratively observed in the maximum intensity projection images of the same patient.

The second reader (a nonspecific radiologist with 2 years of experience) detected centriacinar nodules in 12 (22.6%) of 53 patients on conventional CT images and centriacinar nodules in 48 (90.6%) patients on MIP images (Table 2). When the first and second readers were compared in the detection rate of nodules in the evaluation of conventional images, the first reader was able to detect nodules at a statistically significant rate ( $p < 0.001$ ). In the evaluation of MIP images, a comparison of the first and second readers in the detection rate of nodules could not be made statistically because the first reader detected all nodules at a higher rate in MIP images. For the first reader, a statistical comparison could not be made in the detection of nodules in conventional and MIP images, as all nodules were detected in MIP images, but an increase in the detection rate of nodules in MIP images was observed. In the comparison of conventional and MIP images, it was observed that the detection rate of nodules for the second reader was statistically significantly higher in MIP images ( $p < 0.001$ ).

Ill-defined centrilobular micronodules were observed in all patients (100%). In addition, areas of ground glass density in 31 (58.4%) patients, mosaic perfusion areas (patch-like hypotenuation areas) in 26 (49%) patients, bronchial wall thickening in 35 (66%) patients, emphysema areas in 30 (56.6%) patients, and subpleural reticulations in 5 (9.4%) patients were observed. In the craniocaudal distribution of the findings, upper-middle zone dominance was observed in 41 (77.3%) patients, while zonal dominance was not detected in 12 (26.7%) patients. It was found that the involvement was bilateral in all patients (100%).

## DISCUSSION

In our study, in which we examined the contribution of MIP images to the diagnostic accuracy in detecting micronodules in diseases such as RB and RB-ILD that form ill-defined

**Table 2.** Detection rates of first and second readers' micronodules on conventional computed tomographic images and maximum intensity projection images.

		Conventional images		MIP images		p-value
		Number	%	Number	%	
First reader	Detected	42	79.2	53	100	Could not be calculated
	Not detected	11	10.8	0	0	
Second reader	Detected	12	22.6	48	90.6	<0.001
	Not detected	41	77.4	5	9.4	

MIP: maximum intensity projection.

micronodules in the lung, we were able to show that MIP images increase the detection rate of radiologists regardless of experience. There are studies in the literature showing that MIP images have a higher rate of detecting nodules<sup>4,7-9</sup>, and the importance of MIP images in detecting especially small nodules has been emphasized<sup>10</sup>. However, we have shown for the first time, independent of the radiologist's experience, that MIP images increase the detectability of micronodules for a specific disease such as RB.

Maximum intensity projection images consist of axial slab volumetric data and have two important advantages. The first is to ensure that nodular structures adjacent to vascular structures are clearly discerned in a single image. Second, although it reduces the number of slices available, it does not lose spatial resolution for a single MIP slab. However, it should not be forgotten that there is data loss in MIP reconstruction. In a study, 5 mm MIP slab thickness and 1 mm HRCT and conventional CT micronodule detection were compared. In this study, MIP images of 5 mm slab thickness detected micronodules at the highest rate with 100% sensitivity<sup>5</sup>. However, in another study, 30 mm slab thickness MIP images were evaluated, and the nodule detection rate decreased due to the superposition of pulmonary vascular structures to the nodules<sup>11</sup>. In our study, we evaluated 10 mm slab thickness MIP images. Both readers detected a higher rate of micronodules in MIP images than in conventional images. A statistically significant increase was found in MIP images, especially for the less experienced radiologist.

In the literature, the classic HRCT image of RB has been described as bronchial wall thickening, ill-defined centrilobular nodules, and ground glass areas<sup>12-14</sup>. Involvement in RB is more prominent in the upper zones. Lung fibrosis and honeycombing are uncommon. Findings are usually observed predominantly in the upper zone. Ground glass areas are bilateral, and patchy involvement is observed<sup>15</sup>. We also found similar findings on conventional CT images. We were able to show the nodules more demonstratively in MIP images. In RB, peripherally located ground-glass densities can be observed in the lower lobes with overlapping findings with DIP, another form of smoking-related bronchiolitis<sup>1</sup>. Due to the presence of ill-defined centrilobular nodules, RB is most often confused with subacute hypersensitivity pneumonia<sup>16</sup>. In differential diagnosis, a strong association between smoking history, nonspecific findings in BAL (lymphocytosis is observed in BAL in hypersensitivity pneumonitis), and the absence of organic antigen exposure is observed.

In some cases, other diseases with micronodular involvement may also be included in the differential diagnosis of RB. In this case, attention is paid to the patient's history, involved lung zone, symmetrical or asymmetrical involvement. In addition, attention is paid to the perilymphatic, centrilobular, and random involvement of micronodules. For example, inorganic material exposure is observed in pneumoconiosis and its subtype silicosis. In pneumoconiosis, the nodules are more sharply circumscribed and symmetrically located in the upper lobes. Nodules are frequently observed in the posterior parts of the lung. In miliary tuberculosis, unlike RB, the nodules are randomly distributed and all lobes are uniformly affected. In sarcoidosis, nodules are observed in the perilymphatic region and there is asymmetric involvement<sup>17</sup>.

A strong relationship between RB and smoking is mentioned in the literature<sup>1,12-14</sup>. All of our patients have a strong smoking history. However, in the literature, besides smoking, soldering smoke, diesel smoke, and fiberglass are also included in the etiology<sup>18,19</sup>.

The limitations of our study are as follows: the patients were not confirmed by biopsy, the number of patients studied was low, the number of radiologists who evaluated them was low, and MIP images with a thickness of 5 mm slabs were not studied in the search for nodules.

## CONCLUSION

In patients presenting with a micronodular pattern such as RB, MIP images increase the detectability of micronodules independently of the experience of the radiologist. The inclusion of MIP images in the protocol will increase the accuracy of diagnosis when evaluating the HRCTs of the cases in which micronodules are investigated. We hope that the number of studies supporting our study will increase and the contribution of other advanced reconstruction techniques to the diagnosis of lung diseases will be investigated.

## AVAILABILITY OF DATA

The datasets used and/or analyzed during this study are available from the corresponding author on reasonable request.

## AUTHORS' CONTRIBUTIONS

**HAK:** Conceptualization, Data curation, Writing – original draft, Writing – review & editing. **MB:** Conceptualization, Data curation, Supervision. **EG:** Formal Analysis, Supervision.

## REFERENCES

1. Ryu JH, Myers JL, Capizzi SA, Douglas WW, Vassallo R, Decker PA. Desquamative interstitial pneumonia and respiratory bronchiolitis-associated interstitial lung disease. *Chest*. 2005;127(1):178-84. <https://doi.org/10.1378/chest.127.1.178>
2. Niewoehner DE, Kleinerman J, Rice DB. Pathologic changes in the peripheral airways of young cigarette smokers. *N Engl J Med*. 1974;291(15):755-8. <https://doi.org/10.1056/NEJM197410102911503>
3. Park JS, Brown KK, Tuder RM, Hale VA, King TE, Lynch DA. Respiratory bronchiolitis-associated interstitial lung disease: radiologic features with clinical and pathologic correlation. *J Comput Assist Tomogr*. 2002;26(1):13-20. <https://doi.org/10.1097/00004728-200201000-00003>
4. Jankowski A, Martinelli T, Timsit JF, Brambilla C, Thony F, Coulomb M, et al. Pulmonary nodule detection on MDCT images: evaluation of diagnostic performance using thin axial images, maximum intensity projections, and computer-assisted detection. *Eur Radiol*. 2007;17(12):3148-56. <https://doi.org/10.1007/s00330-007-0727-6>
5. Remy-Jardin M, Remy J, Artaud D, Deschildre F, Duhamel A. Diffuse infiltrative lung disease: clinical value of sliding-thin-slab maximum intensity projection CT scans in the detection of mild micronodular patterns. *Radiology*. 1996;200(2):333-9. <https://doi.org/10.1148/radiology.200.2.8685322>
6. Remy J, Remy-Jardin M, Artaud D, Fribourg M. Multiplanar and three-dimensional reconstruction techniques in CT: impact on chest diseases. *Eur Radiol*. 1998;8(3):335-51. <https://doi.org/10.1007/s003300050391>
7. Cody DD. AAPM/RSNA physics tutorial for residents: topics in CT. Image processing in CT. *Radiographics*. 2002;22(5):1255-68. <https://doi.org/10.1148/radiographics.22.5.g02se041255>
8. Valencia R, Denecke T, Lehmkuhl L, Fischbach F, Felix R, Knollmann F. Value of axial and coronal maximum intensity projection (MIP) images in the detection of pulmonary nodules by multislice spiral CT: comparison with axial 1-mm and 5-mm slices. *Eur Radiol*. 2006;16(2):325-32. <https://doi.org/10.1007/s00330-005-2871-1>
9. Coakley FV, Cohen MD, Johnson MS, Gonin R, Hanna MP. Maximum intensity projection images in the detection of simulated pulmonary nodules by spiral CT. *Br J Radiol*. 1998;71(842):135-40. <https://doi.org/10.1259/bjr.71.842.9579176>
10. Gruden JF, Ouanounou S, Tigges S, Norris SD, Klausner TS. Incremental benefit of maximum-intensity-projection images on observer detection of small pulmonary nodules revealed by multidetector CT. *AJR Am J Roentgenol*. 2002;179(1):149-57. <https://doi.org/10.2214/ajr.179.1.1790149>
11. Diederich S, Lentschig MG, Overbeck TR, Wormanns D, Heindel W. Detection of pulmonary nodules at spiral CT: comparison of maximum intensity projection sliding slabs and single-image reporting. *Eur Radiol*. 2001;11(8):1345-50. <https://doi.org/10.1007/s003300000787>
12. Kumar A, Cherian SV, Vassallo R, Yi ES, Ryu JH. Current concepts in pathogenesis, diagnosis, and management of smoking-related interstitial lung diseases. *Chest*. 2018;154(2):394-408. <https://doi.org/10.1016/j.chest.2017.11.023>
13. Vassallo R. Diffuse lung diseases in cigarette smokers. *Semin Respir Crit Care Med*. 2012;33(5):533-42. <https://doi.org/10.1055/s-0032-1325162>
14. Walsh SL, Nair A, Desai SR. Interstitial lung disease related to smoking: imaging considerations. *Curr Opin Pulm Med*. 2015;21(4):407-16. <https://doi.org/10.1097/MCP.0000000000000178>
15. Mavridou D, Laws D. Respiratory bronchiolitis associated interstitial lung disease (RB-ILD): a case of an acute presentation. *Thorax*. 2004;59(10):910-1. <https://doi.org/10.1136/thx.2003.011080>
16. Park JS, Brown KK, Tuder RM, Hale VA, King TE, Lynch DA. Respiratory bronchiolitis-associated interstitial lung disease: radiologic features with clinical and pathologic correlation. *J Comput Assist Tomogr*. 2002;26(1):13-20. <https://doi.org/10.1097/00004728-200201000-00003>
17. Akgun M, Araz O, Ucar EY, Karaman A, Alper F, Gorguner M, et al. Silicosis appears inevitable among former denim sandblasters: a 4-year follow-up study. *Chest*. 2015;148(3):647-54. <https://doi.org/10.1378/chest.14-2848>
18. Moon J, Bois RM, Colby TV, Hansell DM, Nicholson AG. Clinical significance of respiratory bronchiolitis on open lung biopsy and its relationship to smoking related interstitial lung disease. *Thorax*. 1999;54(11):1009-14. <https://doi.org/10.1136/thx.54.11.1009>
19. Fraig M, Shreesha U, Savici D, Katzenstein AL. Respiratory bronchiolitis: a clinicopathologic study in current smokers, ex-smokers, and never-smokers. *Am J Surg Pathol*. 2002;26(5):647-53. <https://doi.org/10.1097/0000478-200205000-00011>

